Identification of the coastal zone of the central and eastern Gulf of Finland by numerical modeling, measurements, and remote sensing of chlorophyll *a*

Gennadi Lessin · Viktoria Ossipova · Inga Lips · Urmas Raudsepp

Originally published in the journal Hydrobiologia, Volume 629, No. 1, 187–198.
DOI: 10.1007/s10750-009-9770-4

Abstract A combination of numerical modeling results with measurement and satellite imagery data was used during the biologically active period for the determination of the coastal zone extent in the central and eastern Gulf of Finland. Adopting the approach that the coastal zone can be identified by the spatial distribution of biotic parameters, spatial variations and gradients of chlorophyll *a* (chl-*a*) concentrations were analyzed. The results showed that chl-*a* concentrations vary in a wide range over the biologically active period. During heavy blooms, the coastal zone may appear occasionally and depend on the spatial distribution of the bloom. On average, clear limits of the coastal zone could be defined for the central and eastern Gulf of Finland. In the central Gulf of Finland, water and material exchange are rather intensive, and the coastal zone is narrower than in the eastern Gulf. In the easternmost part of the Gulf of Finland, chl-*a* concentrations were permanently high in an area of about 100 km width due to the discharge of the Neva River. The study has shown that gradients of chl-*a* spatial distribution can be applied for determining limits of the coastal zone extent. The standardized gradient of zero is shown to be a threshold separating the coastal zone (standardized gradients > 0) from the open sea (standardized gradients < 0).

Keywords Coastal zone · Numerical modeling · Remote sensing · Chlorophyll *a* · Eutrophication · Gulf of Finland

Introduction

The coastal sea is a primary recipient of nutrients and suspended matter from rivers and other land-based sources. It is also influenced by a number of hydrodynamic processes, for example, currents and upwelling. The complexity and diversity of physical and biological processes may result in sharp gradients of biological and chemical parameters between the coastal zone and the open sea. This makes the coastal sea very important for marine management. Eutrophication, i.e., the increase of nutrient loading, of the Baltic Sea is more obvious in the coastal zone, especially in semi-enclosed bays, lagoons, archipelagoes, and estuaries (Telesh, 2004). Successful measures for eutrophication control require identification of the coastal zone extent.

A variety of criteria have been used for the definition of the coastal zone. These definitions are

Guest editors: J. H. Andersen & D. J. Conley
Eutrophication in Coastal Ecosystems: Selected papers from the Second International Symposium on Research and Management of Eutrophication in Coastal Ecosystems, 20–23 June 2006, Nyborg, Denmark

G. Lessin (✉) · V. Ossipova · I. Lips · U. Raudsepp
Marine Systems Institute, Tallinn University of Technology, Akadeemia tee 21b, 12618 Tallinn, Estonia
e-mail: gennadi@phys.sea.ee

based on geographical extent (European Communities, 2000), geomorphology of the coastal margin (Gazeau et al., 2004), or the extent of river influence (Artioli et al., 2005). However, from the marine management point of view, it is more appropriate to define the coastal zone in terms of biotic distributions and processes, because these are not always aligned with the abiotic structure of nearshore areas (Gibbs et al., 2006).

This study aims at identifying the coastal zone and determining its extent in the central and eastern Gulf of Finland during the biologically active period by combining the results of numerical modeling with measurements and satellite imagery data. Spatial variations and gradients of chl-*a* concentration were analyzed following the approach that the coastal zone can be identified from the spatial distribution and magnitude of gradients of biotic parameters (Lessin & Raudsepp, 2007). It is hypothesized that chl-*a* concentrations are higher in the coastal sea compared with the open sea and that this pattern persists over a prolonged period. The Gulf of Finland is an elongated estuary (Fig. 1a) of the Baltic Sea with a mean depth of 37 m and a maximum depth of 123 m. The western part of the Gulf is directly connected to the Baltic Proper. The eastern part receives the largest single freshwater inflow to the Baltic Sea—the Neva River (Alenius et al., 1998).

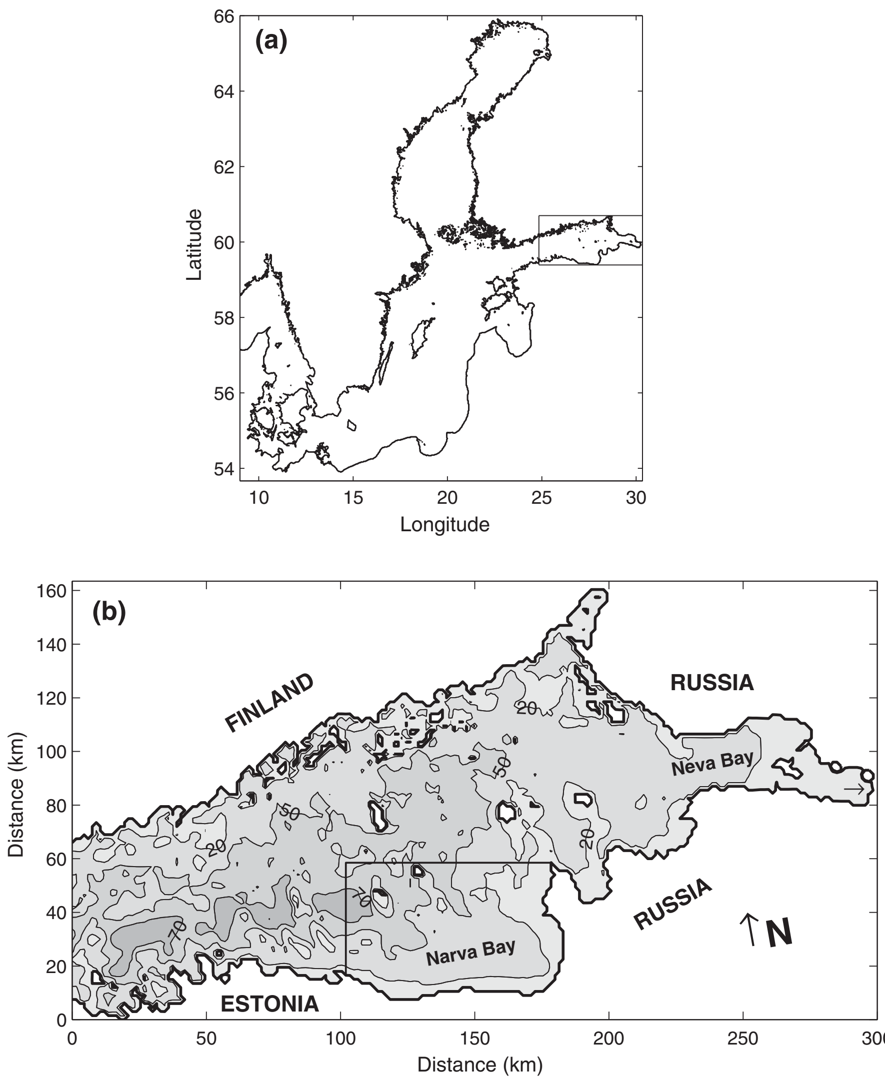

Fig. 1 The Baltic Sea area (**a**) and the model domain covering the central and eastern parts of the Gulf of Finland, with the *x*- and *y*-axes showing the distance (km) from the modeling domain origin in the southern Gulf of Finland (**b**). The small arrow points at the Neva River mouth. Limits of Narva Bay defined according to Piirsoo et al. (1992) are shown

Materials and methods

Numerical model

The ecohydrodynamic three-dimensional model MIKE 3 (DHI Water and Environment, 2001) was applied for the central and eastern parts of the Gulf of Finland (Fig. 1b). The basic equations of the hydrodynamic model consist of a mass conservation equation for compressible fluid, non-linear momentum equations in the three main directions, a conservation equation for salinity and temperature, and the equation of state of the seawater (Rasmussen, 1993). The simulations were performed with a hydrostatic model version. The Smagorinsky formulation was used for horizontal eddy viscosity and the $k - \varepsilon$ formulation was used for the vertical turbulent closure model (Burchard et al., 1998; Rasmussen et al., 1999). The main forcing factors included wind stress and heat exchange at the surface, prescribed sea level at the open boundary, and freshwater inflow by rivers. The ecological model includes 11 interdependent state variables: phytoplankton carbon (PC), nitrogen and phosphorus; chl-*a*; zooplankton; detritus carbon, nitrogen and phosphorus; inorganic nitrogen (IN); inorganic phosphorus (IP); and dissolved oxygen. Concentrations of total nitrogen (TN) and total phosphorus (TP) are also calculated. The model implements two phytoplankton groups: diatoms and green algae, which appear in consecutive order in the model. The ecological model describes the relation between available inorganic nutrients and the subsequent phytoplankton growth. The nutrient supply depends on the land-based load and the transport into the area through model open boundaries. The simulation time covered the biologically active period from April 1 to September 30, 2001. The model spatial resolution was 1,500 m horizontally and 2 m vertically, except for the upper layer which was 3 m thick. Model results were stored at 6 h intervals.

The initial temperature (T) and salinity (S) fields were prepared based on a limited number of TS-casts. The initial temperature distribution was assumed to be horizontally uniform while keeping vertical stratification. The salinity values were horizontally interpolated to a model grid using a bilinear interpolation method. The initial concentrations of PC, chl-*a*, and zooplankton were derived from a very limited number of measurements, which only allowed the use of homogeneous concentrations for those variables. The initial concentrations of 0.2 mg l^{-1} were taken for PC and 0.01 mg l^{-1} for chl-*a*. The initial distributions of IN, IP, detritus carbon, detritus nitrogen, detritus phosphorus, and dissolved oxygen were prepared based on a limited amount of measurement data. The data were interpolated onto the model grid using objective analysis (Lessin & Raudsepp, 2006).

The boundary conditions for ecological variables were prepared based on data from three or four locations, where samples were collected at standard depth. The measurements were performed once per month in April, May, and September and twice per month in June, July, and August. The measured values were interpolated onto a model grid on the open boundary. An accurate description of the open boundary conditions is of great importance for the correct performance of the model. Figure 2 shows a validation of model results (PC, chl-*a*, TN, TP) at station F3 situated in the vicinity of the open boundary. Although measurement data were very scarce, the comparison gives an indication of a satisfactory description of the open boundary conditions.

A thorough model description and setup as well as model validation results for Narva Bay, in the south-eastern Gulf of Finland, are given by Lessin & Raudsepp (2006) and Lessin et al. (2007).

Measurement data

Measurement data originated from the automatic ferry-box system on the ferry operating between Tallinn and Helsinki (Kanoshina et al., 2003). The water intake and sampling were located at 4–5 m depth and data were collected once per week from April to November 2001. Fluorescence was recorded every 10 s (corresponding to a horizontal resolution of approximately 200 m) during the crossing between Tallinn and Helsinki. During each crossing, water samples were collected from nine sampling locations for laboratory analyses of chl-*a*. The fluorescence values were converted to chl-*a* using a linear regression relationship for each crossing separately.

Satellite imagery

Moderate resolution (1 km/pixel) MODIS/Aqua Level 2 images of chl-*a* for the years 2002 and 2003 were obtained from the OceanColor website

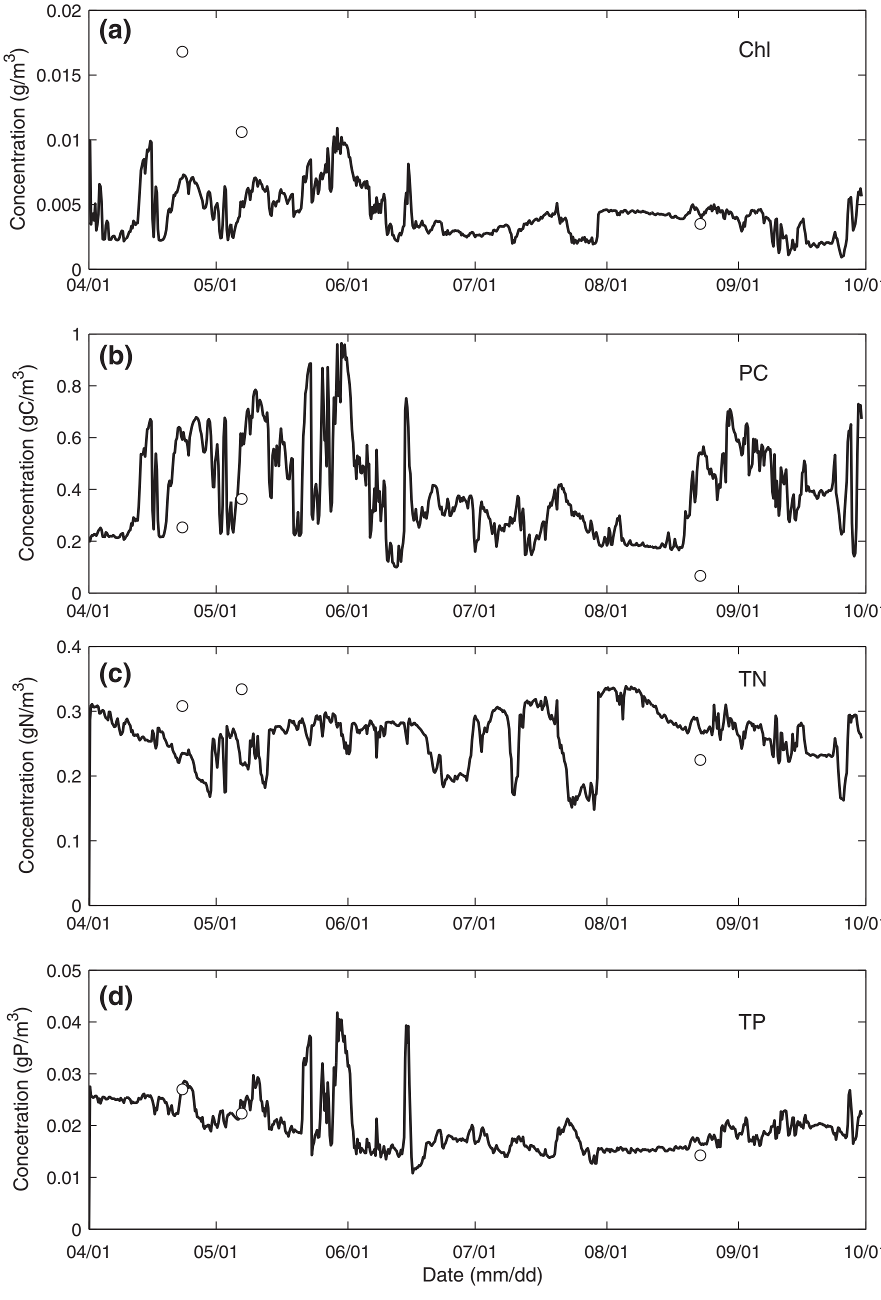

Fig. 2 Modeled (*line*) and observed (*dots*) values for chl-*a* (**a**) and phytoplankton carbon (**b**) integrated over the upper 1–10 m layer and surface total nitrogen (**c**) and total phosphorus (**d**) at station F3 in the vicinity of model open boundary

(http://oceancolor.gsfc.nasa.gov/). Due to frequent cloud cover, good quality satellite images for the Gulf of Finland are rare. In total, 40 images that cover the biologically active period were chosen for the analysis. The bio-optical MODIS algorithms with their present standard parameterization are inappropriate for applications in the Baltic Sea because the standard algorithm (MODIS OC3) usually tends to overestimate chlorophyll concentration, especially during heavy cyanobacterial blooms (Reinart & Kutser, 2006). Therefore, the regional Baltic version of the MODIS chlor_a_2 algorithm (Darecki & Stramski, 2004) was applied for retrieving the chl-*a* concentrations. During image processing, the shallow water and land flags were used for reducing their influence on the chl-*a* concentration in the coastal zone.

Results

The model results on chl-*a* distribution in the surface layer were averaged over the period from April 1 to September 30, which spans the biologically active period in the Gulf of Finland (Fig. 3). Chl-*a* concentrations were relatively high, both close to the coast and offshore in the western part of the model domain (corresponding to the central Gulf of Finland). Along the Estonian coast, the area of high chl-*a* concentration becomes narrower toward the east. In the central part of the model domain (the eastern Gulf of Finland), a distinctive chlorophyll-rich water belt was formed along the southern coast of the Gulf. Chl-*a* concentrations in the central and eastern Gulf decreased rapidly toward offshore, where a vast area of lower chl-*a* was found. An area of increased chl-*a* concentration was also seen along the Finnish coast. Chl-*a* values started to increase in the eastern part of the model domain and were the highest in the Neva Bay due to the discharge of the Neva River.

Because chl-*a* concentrations are considerably higher during the spring bloom period than during the rest of the year, model results were averaged over the period from June 15 to September 30 to exclude the effect of the spring bloom. Mean chl-*a* distribution for the summer period showed a similar pattern, although concentrations were lower (not shown).

For four transects across the Gulf of Finland (Fig. 4), modeled chl-*a* concentrations averaged over

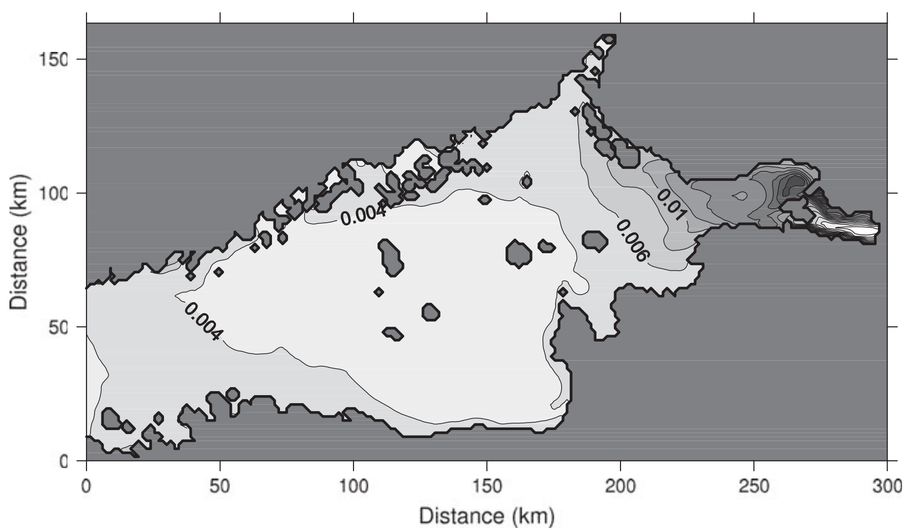

Fig. 3 Modeled average surface chl-*a* concentrations (mg l^{-1})

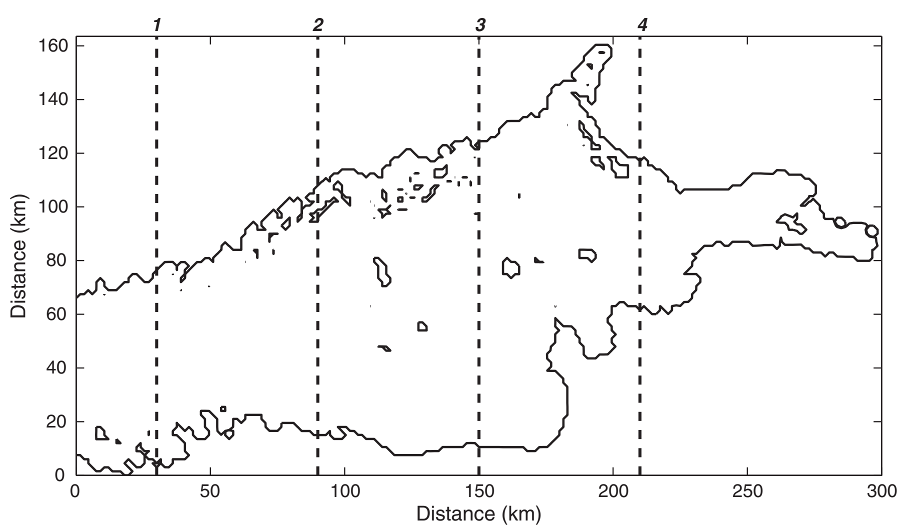

Fig. 4 Location of the transects used for the analysis of modeled extent of the coastal zone

the whole period and the summer period are shown in Fig. 5. High chl-*a* concentrations at the coast and a rather rapid decrease to the open sea values can be seen at the southern coast of the Gulf of Finland on transects 2 and 3 and at the northern coast on transect 1. The latter distribution almost disappears during the summer period. The width of the coastal zone could be estimated at about 5–8 km. The chl-*a* distribution on transect 4 is considerably different. In general, the concentrations were higher in the northern part than in the southern part. The highest concentrations were found offshore, about 12 km from the northern coast with a local minimum in the central part. Model results showed that distribution of chl-*a* at this transect followed the outflow pattern of the Neva River.

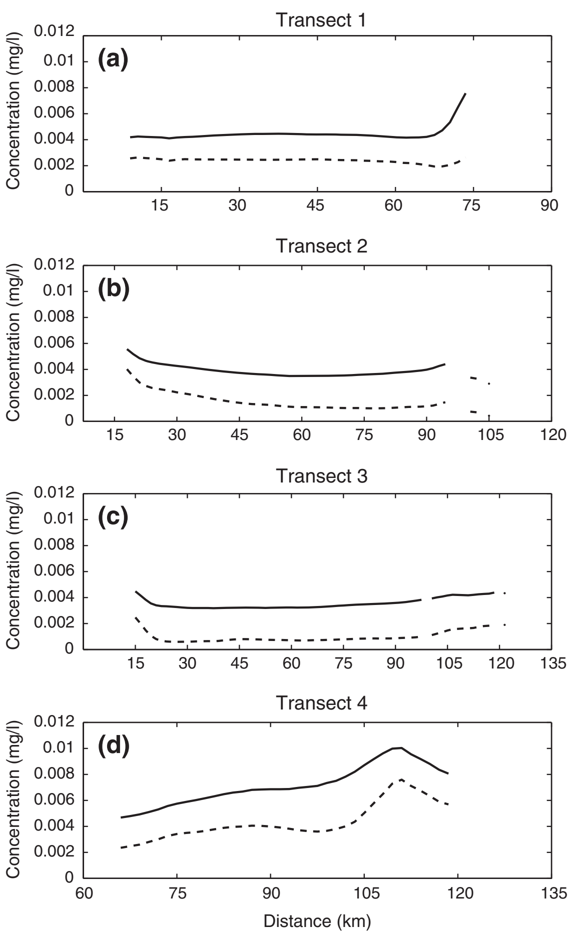

Fig. 5 Mean-modeled concentrations (mg l^{-1}) of chl-*a* along transects 1 (**a**), 2 (**b**), 3 (**c**), and 4 (**d**). *Solid lines* show the entire modeled period; *dashed lines* show the summer period. The *x*-axis shows the distance (km) from the modeling domain origin in the southern Gulf of Finland

The temporally averaged distribution of measured chl-*a* was calculated for two periods: from April 1 to September 30 and from June 15 to September 30, 2001. The chl-*a* values on each transect were interpolated on a regular grid with respect to geographical latitude to facilitate averaging. The measurements clearly show increased chl-*a* concentrations close to both coasts of the central Gulf of Finland (Fig. 6). (Please recall that the Tallinn–Helsinki ferry crossing is situated at the model open boundary.) The chl-*a* concentration for the whole period is about 0.012–0.013 mg l^{-1} close to the coast and drops to 0.01 mg l^{-1} within 2–3 km from the coast (Fig. 6a). The standard deviation increases from 0.005 mg l^{-1} at the southern coast of the Gulf of Finland to 0.01 mg l^{-1} at the northern coast. The high chl-*a* concentrations at the coast and their rapid decrease toward offshore are clearly represented when the effect of the spring bloom is excluded (Fig. 6b). Chl-*a* concentrations were about 0.01 mg l^{-1} near the shore and 0.005 mg l^{-1} in the open sea. Also, the variability of chl-*a* concentrations

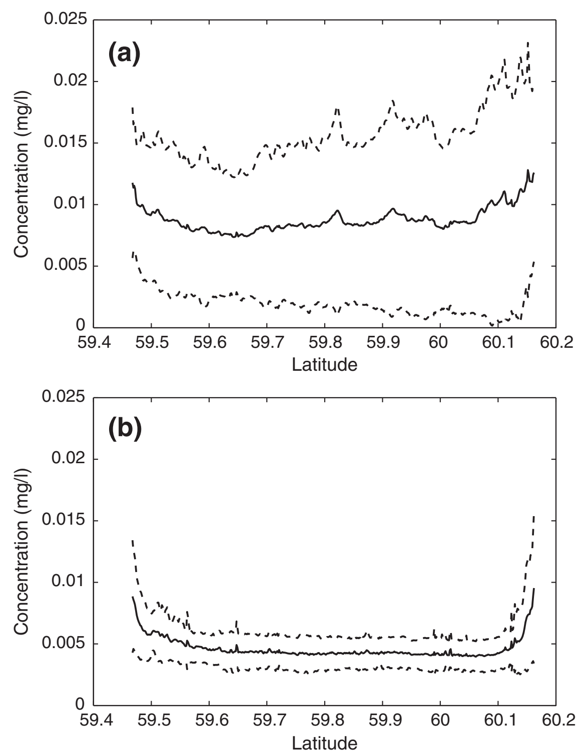

Fig. 6 Measurement data on chl-*a* concentrations (mg l^{-1}) for the entire period (**a**) and for the summer period (**b**). *Solid lines* show average values; *dashed lines* show upper and lower limits of the standard deviation

was lower offshore ($\sim$0.003 mg l^{-1}) than near the coasts (up to $\sim$0.013 mg l^{-1}).

A comparison of modeled and measured mean chl-*a* concentrations in the central Gulf of Finland indicates that modeled chl-*a* values are underestimated approximately two times. This can be explained by the fact that measurements were performed at 4–5 m depth, where chlorophyll concentrations are usually higher than near the surface (e.g., Kononen et al., 1998).

The temporal variability of the modeled surface layer chl-*a* concentration was analyzed on the four transects across the Gulf of Finland. The chl-*a* values on each transect and time instant were divided by the maximum value on that transect, as the main focus of our study was to analyze the chl-*a* distribution in the coastal area relative to the open sea, i.e., across the Gulf. In general, temporal variations of relative surface chl-*a* are different in different parts of the Gulf of Finland (Fig. 7). In the central Gulf (transect 1), a relatively high chl-*a* concentration was present in a 5–15 km belt near the Finnish coast from the second week of April until July. Later on, the concentrations were often higher in offshore than close to the coast. However, a broad area of elevated chl-*a* concentration formed near the Estonian coast in September. Moving further to the east, i.e., transects 2 and 3, chl-*a* concentrations were rather uniform across the Gulf until May. A broad area (about 20–30 km) of increased chl-*a* concentration formed at the Finnish coast, which existed until the end of August, disappearing occasionally. At the Estonian coast, a narrow zone of high chl-*a* concentration could be identified from the beginning of July. The width of this zone was about 5–10 km, except at transect 2, where it broadened up to $\sim$45 km in September. Close to Neva Bay, in the eastern Gulf of Finland (transect 4), concentrations of chl-*a* were high in the northern part of the Gulf, but at some distance from the shore. The chl-*a* concentration was lower in the southern part of the Gulf of Finland compared with the northern part.

All the available satellite data for chl-*a* distribution over the study area (40 images) were averaged monthly. These data were then averaged to produce a composite image (Fig. 8). Although the modeled year is 2001, using images from 2002 and 2003 allows the results of numerical modeling to be generalized. In order to eliminate the effect of the spring bloom, averaging of satellite data for the summer months only was performed. Although showing lower concentrations, the overall spatial distribution of chl-*a* remained similar (not shown).

The composite image (Fig. 8) revealed a belt of increased chl-*a* concentrations along the coasts of the Gulf of Finland. This zone was narrow, but clearly discernible along the northern coast of the Gulf. Along the southern coast, a belt of higher concentrations steadily broadened from the westernmost part of the study area toward the south-eastern part (Narva Bay). Concentrations dropped rapidly toward the offshore where a region of low and uniform chl-*a* occurred. The easternmost area of the Gulf (Neva Bay) was characterized by high concentrations of chl-*a* as an effect of the Neva River discharge. The strong patchiness in chl-*a* distribution in the northeastern part of the Gulf can also be attributed to the effect of Neva River action.

The increased chl-*a* concentrations were found along or in the vicinity of the coast both in the model results and in satellite data. Therefore, in order to discern limits of the coastal zone, a calculation of the spatial gradient of chl-*a* concentrations was applied for both mean-modeled and composite satellite data. Because the relative distribution of gradients is of particular interest for the identification of the coastal zone, standardized gradients were calculated as $g_s = (g - \bar{g})/\sigma_g$, where g is the gradient, $\bar{g}$ is the mean and σ_g is the standard deviation of the gradient calculated over the Gulf of Finland. Both the model (Fig. 9) and satellite (Fig. 10) data showed similar results. The area of positive gradients (presented in black in the figures) generally formed a narrow belt along the coast of the Gulf of Finland. In Neva Bay, the area of positive gradients propagated far offshore westwards. Thus, a standardized gradient of zero can serve as a threshold value delimiting the coastal zone (standardized gradients > 0) from the open Gulf (standardized gradients < 0). Moreover, the coastal zone is characterized by a rapid decline in gradient values toward the offshore where gradients were rather uniform.

Discussion

An application of chl-*a* distribution for the identification of the coastal zone shows that this zone is more a dynamic than a rigid concept. Chl-*a* concentration

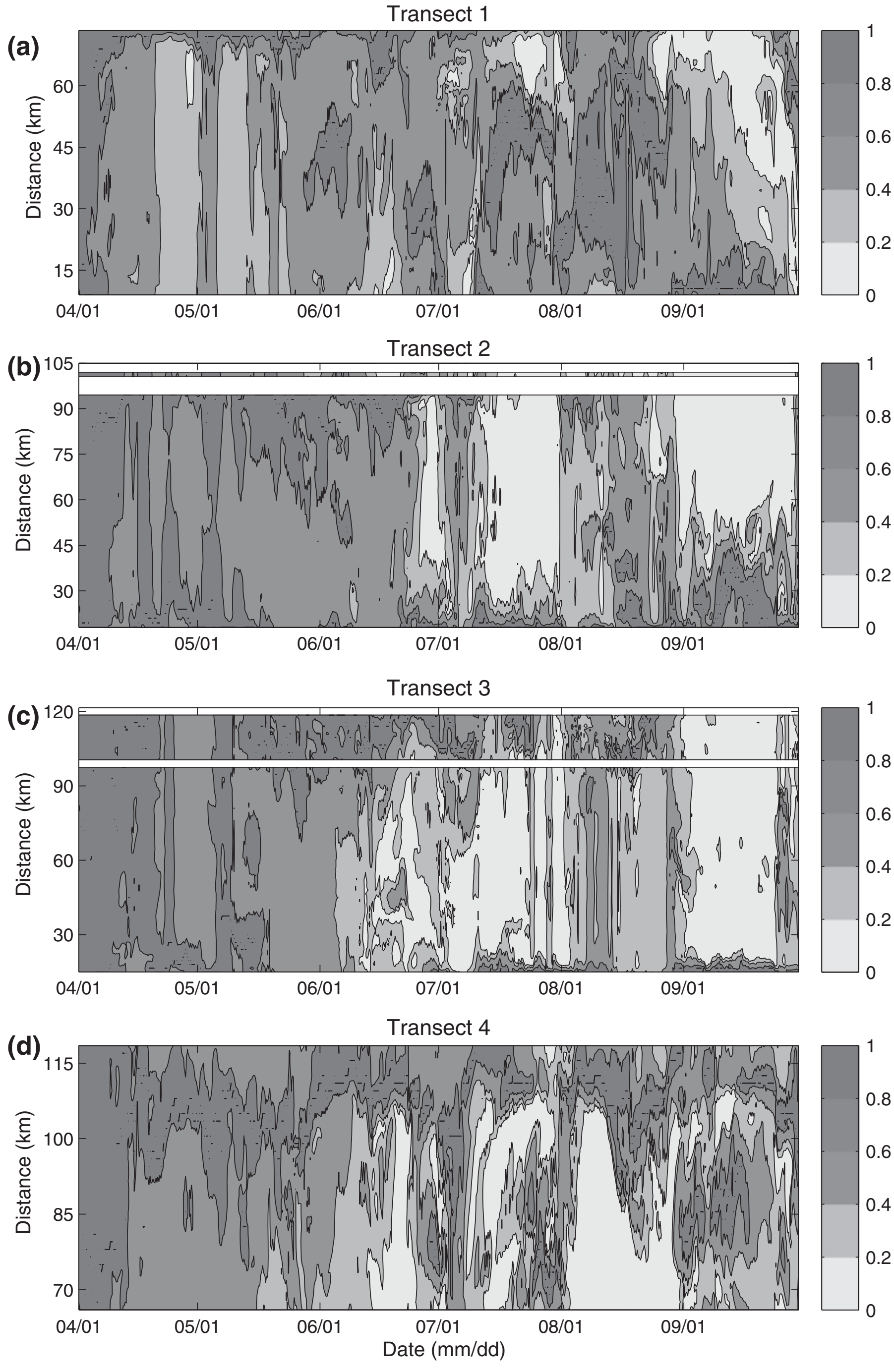

Fig. 7 Modeled normalized temporal variability of chl-*a* concentrations (see key on the right side of the figure) along transects 1 (**A**), 2 (**B**), 3 (**C**), and 4 (**D**). The *y*-axis shows the distance (km) from the modeling domain origin in the southern Gulf of Finland

varies in a broad range over the biologically active season. In the Gulf of Finland, high chl-*a* values are present during the spring diatom bloom and summer cyanobacterial bloom. The latter shows considerable inter-annual variations (Kahru et al., 1995; Laanemets et al., 2006). Ignoring seasonal variations to some extent, the possibility to identify the coastal zone as the area of elevated chl-*a* concentration compared to offshore regions was investigated. The results showed higher concentrations and positive standardized

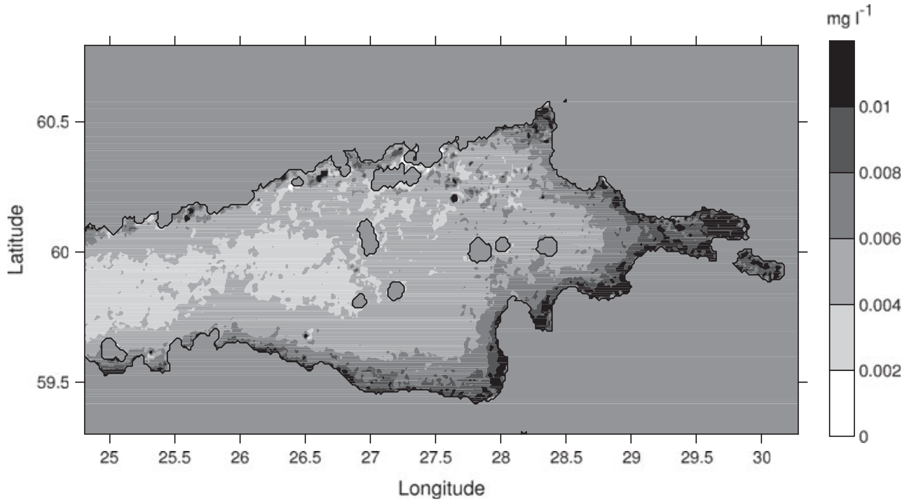

Fig. 8 Composite satellite image of chl-*a* distribution (mg l^{-1}) in the Gulf of Finland

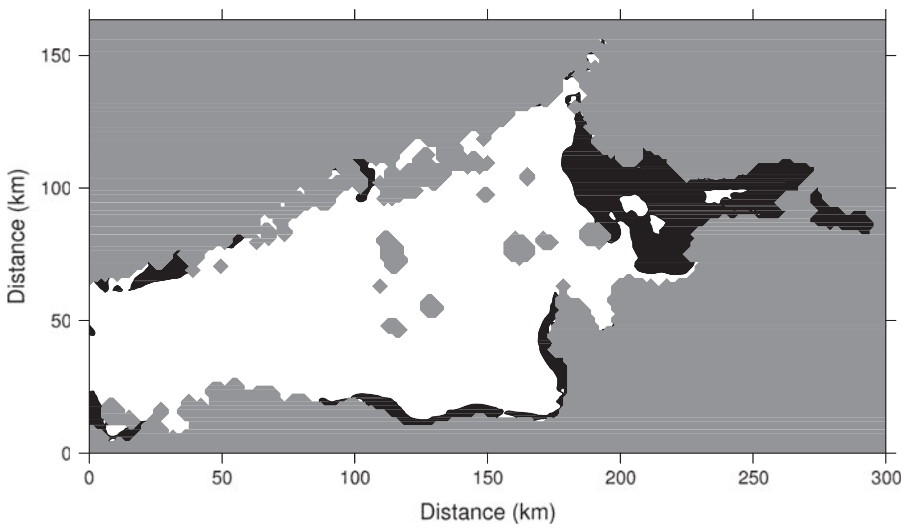

Fig. 9 Standardized gradient of mean modeled surface chl-*a* concentration in the Gulf of Finland. The area of positive gradient values is shown in black

gradients of chl-*a* along the coast of the Gulf of Finland, while offshore concentrations were lower and standardized gradients were negative.

Clear limits of the coastal zone could be identified in the central and eastern Gulf of Finland. Although water and material exchange between the coastal zone and the open sea is rather intensive in the central Gulf of Finland and coastal upwelling filaments may extend far offshore (Vahtera et al., 2005), composite satellite images and measurement data showed relatively low offshore concentrations and the presence of a narrow coastal zone. According to the measurement data, on average during the biologically active season, a chl-*a* concentration of 0.01 mg l^{-1} delimits the outer border of the coastal zone in the central Gulf of Finland. Taking into account the difference between model and measurements, in the model a chl-*a* concentration of 0.005 mg l^{-1} is the threshold value indicating the limit of the coastal zone. The same concentration has been shown by the satellite data. A narrow belt of positive standardized gradients along the Estonian coast in the central Gulf is reproduced

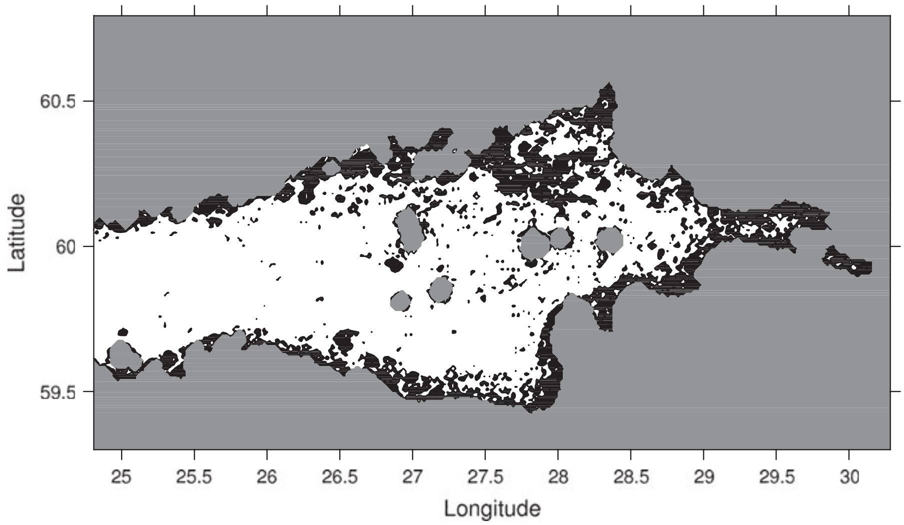

Fig. 10 Standardized gradient of surface chl-*a* concentration in the Gulf of Finland derived from satellite data. The area of positive gradient values is shown in black

better in the satellite data than in the model (this can be partly explained by the higher resolution of satellite images compared with the model grid). Gradients near the northern coast are reproduced similarly by both model and satellite data.

In the eastern Gulf, both satellite and model similarly reproduced the chl-*a* distribution along the southern coast. In the model, a coastal zone of 5–20 km width with a chl-*a* concentration above 0.004 mg l^{-1} is discernible from longitude 26°E toward the east. Satellite data indicate a higher chl-*a* concentration in this zone (0.008 mg l^{-1}). Nevertheless, the limits of the area of positive standardized gradients correspond well in both methods. The northern coast of the eastern Gulf can be characterized by chl-*a* concentrations of 0.004–0.006 mg l^{-1} by both modeling and satellite data. However, the satellite image showed high patchiness in that region, and it also produced a vast area of positive gradients. This distribution pattern can be explained by the mean surface layer circulation to some extent. Mean currents between 4 and 10 cm s^{-1} occur to the east along the southern shore, while they are mainly <4 cm s^{-1} and offshore near the northern coast (Andrejev et al., 2004).

The chl-*a* concentrations were permanently high in the easternmost region of the Gulf of Finland (>0.008 mg l^{-1}). Positive gradients of chl-*a* in the Neva Bay can be seen in both the satellite data and model. In the latter, the area of high chl-*a* and strong positive gradients propagates slightly further. The coastal zone in the easternmost part of the study area could be defined as the region about 100-km wide from the Neva River mouth, following the definition of Artioli et al. (2005).

Temporal variations of chl-*a* concentration emphasize the dynamic nature of the coastal zone. During heavy blooms, i.e., the spring bloom and late summer cyanobacterial bloom in this case, the coastal zone may appear occasionally depending on the spatial distribution of the bloom. Due to the elongated shape of the Gulf of Finland, the cross-Gulf relative chl-*a* distribution was rather uniform during the spring bloom. The late summer cyanobacterial bloom is not directly taken into account in the model. Comparing the cross-Gulf relative chl-*a* concentrations on transects 1–3 shows that the coastal zone can be clearly identified in the summer and autumn on transects 2 and 3. Relatively high modeled chl-*a* concentrations in the offshore area along the western transect during the summer period could be the result of high chl-*a* concentrations prescribed at the model open boundary that are transported eastwards by model currents. Measured data from 2001 on the ferry line between Tallinn and Helsinki give a hint that even in the case of the summer cyanobacterial bloom, a narrow coastal zone of about several kilometers exists. Laanemets et al. (2006) showed that the cyanobacterial bloom was smaller in the central Gulf of Finland in 2001 than in 2002, but still significant.

Conclusion

A combined analysis of numerical modeling results, measurements, and satellite imagery data was used to study the existence of the coastal zone through variations of chl-*a* concentration in the central and eastern parts of the Gulf of Finland. By following the approach that the chl-*a* concentration is elevated near shore compared to the open sea, it was shown that the coastal zone is a dynamic concept that varies in time and space under the influence of ecohydrodynamic processes.

An analysis of the results of the chl-*a* distribution allowed the study area to be divided into two distinct parts: the central and eastern Gulf where high concentrations were present close to the coast; and Neva Bay which is usually high in chl-*a* due to the Neva River influence. It was shown that near the coast, areas of positive standardized gradients of chl-*a* concentration are found. The gradients are highest adjacent to the coast and drop rapidly toward the offshore, where gradients are negative and more or less uniform. Taking that into consideration, a standardized gradient of zero is a suitable criterion for setting the outer boundary of the coastal zone. Model results have shown that in the Neva Bay, elevated chl-*a* values can be found several kilometers offshore. Therefore, it is more appropriate to define the coastal zone in Neva Bay by the area of river influence. Using gradients of the distribution of ecological parameters for defining the extent of the coastal zone has been proposed by Lessin & Raudsepp (2007). Although in the current study different methods showed slightly different chl-*a* concentrations for the same regions, the limits of the coastal zone denoted by the magnitude of standardized gradients were similar.

Acknowledgments This work was partially supported by Estonian Science Foundation research grants numbers 5596 and 7581 and Danish EPA project EISEMM. Measured chl-*a* values in a transect between Tallinn and Helsinki were provided by the Alg@line project.

References

Alenius, P., K. Myrberg & A. Nekrasov, 1998. The physical oceanography of the Gulf of Finland: a review. Boreal Environment Research 3: 97–125.

Andrejev, O., K. Myrberg, P. Alenius & P. A. Lundberg, 2004. Mean circulation and water exchange in the Gulf of Finland—a study based on three-dimensional modelling. Boreal Environment Research 9: 1–16.

Artioli, Y., G. Bendoricchio & L. Palmeri, 2005. Defining and modelling the coastal zone affected by the Po River (Italy). Ecological Modelling 184: 55–68.

Burchard, H., O. Petersen & T. P. Rippeth, 1998. Comparing the performance of the Mellor–Yamada and the k-ε two-equation turbulence models. Journal of Geophysical Research 103: 10.543–10.554.

Darecki, M. & D. Stramski, 2004. An evaluation of MODIS and SeaWiFS bio-optical algorithms in the Baltic Sea. Remote Sensing of Environment 89: 326–350.

DHI Water and Environment, 2001. MIKE 3: environmental hydraulics. DHI Software User Guide, Documentation and Reference Manual.

European Communities, 2000. Directive 2000/60/EC of the European Parliament and of the Council of 23 October 2002 establishing a framework for Community action in the field of water policy. Official Journal of the European Communities, L327, 22 December 2000.

Gazeau, F., S. V. Smith, B. Gentili, M. Frankignoulle & J.-P. Gattuso, 2004. The European coastal zone: characterization and first assessment of ecosystem metabolism. Estuarine, Coastal and Shelf Science 60: 673–694.

Gibbs, M. T., A. J. Hobday, B. Sanderson & C. L. Hewitt, 2006. Defining the seaward extent of New Zealand's coastal zone. Estuarine, Coastal and Shelf Science 66: 240–254.

Kahru, M., B. Hakansson & O. Rud, 1995. Distributions of the sea-surface temperature fronts in the Baltic Sea as derived from satellite imagery. Continental Shelf Research 15: 663–679.

Kanoshina, I., U. Lips & J.-M. Leppanen, 2003. The influence of weather conditions (temperature and wind) on cyanobacterial bloom development in the Gulf of Finland (Baltic Sea). Harmful Algae 2: 29–41.

Kononen, K., S. Hällfors, M. Kokkonen, H. Kuosa, J. Laanemets, J. Pavelson & R. Autio, 1998. Development of a subsurface chlorophyll maximum at the entrance to the Gulf of Finland, Baltic Sea. Limnology and Oceanography 43: 1089–1106.

Laanemets, J., M.-J. Lilover, U. Raudsepp, R. Autio, E. Vahtera, I. Lips & U. Lips, 2006. A fuzzy logic model to describe the cyanobacteria *Nodularia spumigena* blooms in the Gulf of Finland, Baltic Sea. Hydrobiologia 554: 31–45.

Lessin, G. & U. Raudsepp, 2006. Water quality assessment using integrated modeling and monitoring in Narva Bay, Gulf of Finland. Environmental Modeling and Assessment 11: 315–332.

Lessin, G. & U. Raudsepp, 2007. Modelling the spatial distribution of phytoplankton and inorganic nitrogen in Narva Bay, southeastern Gulf of Finland, in the biologically active period. Ecological Modelling 201: 348–358.

Lessin, G., I. Lips & U. Raudsepp, 2007. Modelling nitrogen and phosphorus limitation on phytoplankton growth in Narva Bay, south-eastern Gulf of Finland. Oceanologia 49: 259–276.

Piirsoo, K., V. Porgasaar & M. Viik, 1992. Environmental conditions, phytoplankton and chlorophyll *a* in the Narva Bay (the southern part of the Gulf of Finland). Proceedings of the Estonian Academy of Sciences. Biology 41: 149–161.

Rasmussen, E. B., 1993. Three-dimensional hydrodynamic models. Sect. 3.1 hydrodynamic models. In Abbot, M. B. & N. A. Price (eds), Coastal, Estuarine and Harbour Engineer's Reference Book. Chapman and Hall, London: 109–116.

Rasmussen, E. B., J. Pietrzak & R. Brandt, 1999. A coupled ice-ocean model for the Greenland, Iceland and Norwegian Seas. Deep-Sea Research Part II 46: 1169–1198.

Reinart, A. & T. Kutser, 2006. Comparison of different satellite sensors in detecting cyanobacterial bloom events in the Baltic Sea. Remote Sensing of Environment 102: 74–85.

Telesh, V. I., 2004. Plankton of the Baltic estuarine ecosystems with emphasis on Neva Estuary: a review of present knowledge and research perspectives. Marine Pollution Bulletin 49: 206–219.

Vahtera, E., J. Laanemets, J. Pavelson, M. Huttunen & K. Kononen, 2005. Effect of upwelling on the pelagic environment and bloom-forming cyanobacteria in the western Gulf of Finland, Baltic Sea. Journal of Marine Systems 58: 67–82.